PAPER

Spin crossover in dinuclear iron(II) complexes bridged by bis-bipyridine ligands: dimer effects on electronic structure, spectroscopic properties and spin-state switching†

Clara Trommer,[a] Eike Kuhlemann,[a] Tobias A. Engesser, [ID][a] Marcel Walter,[b] Sangeeta Thakur, [ID][b] Wolfgang Kuch [ID] *[b] and Felix Tuczek [ID] *[a]

Inspired by the well-studied mononuclear spin crossover compound [Fe(H$_2$B(pz)$_2$)$_2$(bipy)], the bipyridine-based bisbidentate ligands 1,2-di(2,2′-bipyridin-5-yl)ethyne (ac(bipy)$_2$) and 1,4-di(2,2′-bipyridine-5-yl)-3,5-dimethoxybenzene (Ph(OMe)$_2$(bipy)$_2$) are used to bridge two [Fe(H$_2$B(pz)$_2$)$_2$] units, leading to the charge-neutral dinuclear iron(II) compounds [{Fe(H$_2$B(pz)$_2$)$_2$}$_2$ μ-(ac(bipy)$_2$)] (**1**) and [{Fe(H$_2$B(pz)$_2$)$_2$}$_2$ μ-(Ph(OMe)$_2$(bipy)$_2$)] (**2**), respectively. The spin-crossover properties of these molecules are investigated by temperature-dependent PPMS measurements, Mössbauer, vibrational and UV/Vis spectroscopy as well as X-ray absorption spectroscopy. While compound **1** undergoes complete SCO with $T_{1/2}$ = 125 K, an incomplete spin transition is observed for **2** with an inflection point at 152 K and a remaining high-spin fraction of 40% below 65 K. The spin transitions of the dinuclear compounds are also more gradual than for the parent compound [Fe(H$_2$B(pz)$_2$)$_2$(bipy)]. This is attributed to steric hindrance between the molecules, limiting intermolecular interactions such as π−π-stacking.

Introduction

Spin crossover (SCO) is a phenomenon whereby the spin state of a 3d metal complex changes between the low spin (LS) and the high spin (HS) state, made possible by a suitable ligand field splitting. This process can be stimulated by, *e.g.*, temperature, light or pressure.[1,2] Iron(II) compounds constitute a major field in SCO research, switching between the diamagnetic LS state with S = 0 and the paramagnetic HS state with S = 2.[1–3] During the spin transition not only magnetic, but also electronic and optical properties of the molecule change, making these compounds promising candidates for applications in electronic devices, switching units or sensors.[4,5]

If cooperative effects are present, the SCO becomes abrupt and may show hysteresis and thereby bistability. This is in general the case when the SCO centres are subject to intra- or intermolecular interactions.[6–8] Notably, SCO also goes along with a change in Fe–N bond length that may force surrounding

SCO centres into the same spin state. This is an important source of cooperativity in mononuclear spin-crossover compounds.[9–11] In addition, strong cooperative effects are observed in polynuclear compounds or coordination networks.[8,12,13] Bistability as a result of cooperativity is of particular interest regarding possible applications.[4,14] In order to obtain insight into the emergence of cooperative effects we envisaged the synthesis of polynuclear iron(II) SCO complexes having 2,2′-bipyridine as bridging unit for the build-up of a linear chain wherein each 2,2′-bipyridine coordinates a charge-neutral [Fe(H$_2$B(pz)$_2$)$_2$] (pz = 1*H*-pyrazole) unit. We chose [Fe(H$_2$B(pz)$_2$)$_2$] as building block because of the well-studied SCO properties of a large number of compounds having the constitution [Fe(H$_2$B(pz)$_2$)$_2$(L)], L = 2,2′-bipyridine (bipy) or other diamine ligands. The parent complex [Fe(H$_2$B(pz)$_2$)$_2$(bipy)] exhibits an abrupt SCO with $T_{1/2}$ = 161 K as shown by magnetic measurements as well as UV/Vis and vibrational spectroscopy, also allowing studies on LIESST.[15,16] This complex and a large group of related compounds have not only been extensively investigated as bulk material, but could also be deposited as thin films to study surface-induced effects on the SCO behaviour.[16–25] In particular, the development of cooperativity in ultrathin layers of [Fe(H$_2$B(pz)$_2$)$_2$(bipy)] on a graphite surface has recently been investigated. Interestingly, the abrupt spin transition of [Fe(H$_2$B(pz)$_2$)$_2$(bipy)] becomes more gradual as the film thickness decreases, indicating that inter-

[a]*Institut für Anorganische Chemie, Christian-Albrechts-Universität zu Kiel, Max-Eyth-Straße 2, D-24118 Kiel, Germany. E-mail: ftuczek@ac.uni-kiel.de*
[b]*Institut für Experimentalphysik, Freie Universität Berlin, Arnimallee 14, D-14195 Berlin, Germany. E-mail: kuch@physik.fu-berlin.de*

molecular interactions, specifically π–π stacking between the aromatic systems of the bipyridine units, contribute to enhanced cooperativity in the bulk material.[19] These findings make it promising to develop polynuclear SCO complexes for studies on cooperative effects.

In the following, we describe the synthesis and characterization of the dinuclear SCO compounds [{Fe(H₂B(pz)₂)₂}₂ μ-(ac(bipy)₂)] (**1**) and [{Fe(H₂B(pz)₂)₂}₂ μ-(Ph((OMe)₂(bipy)₂))] (**2**). In these systems the bipyridine units are connected either by an acetylene or a dimethoxyphenylene unit (Scheme 1). The chosen bridging ligands are synthetically well-established and commonly used for other metal centers like ruthenium.[26–30] The SCO properties of **1** and **2** are investigated by PPMS measurements, Mössbauer spectroscopy and vibrational as well as UV/Vis spectroscopy, also allowing studies on the LIESST-effect for both compounds. Finally, the acetylene-bridged compound **1** is investigated by X-ray absorption spectroscopy.
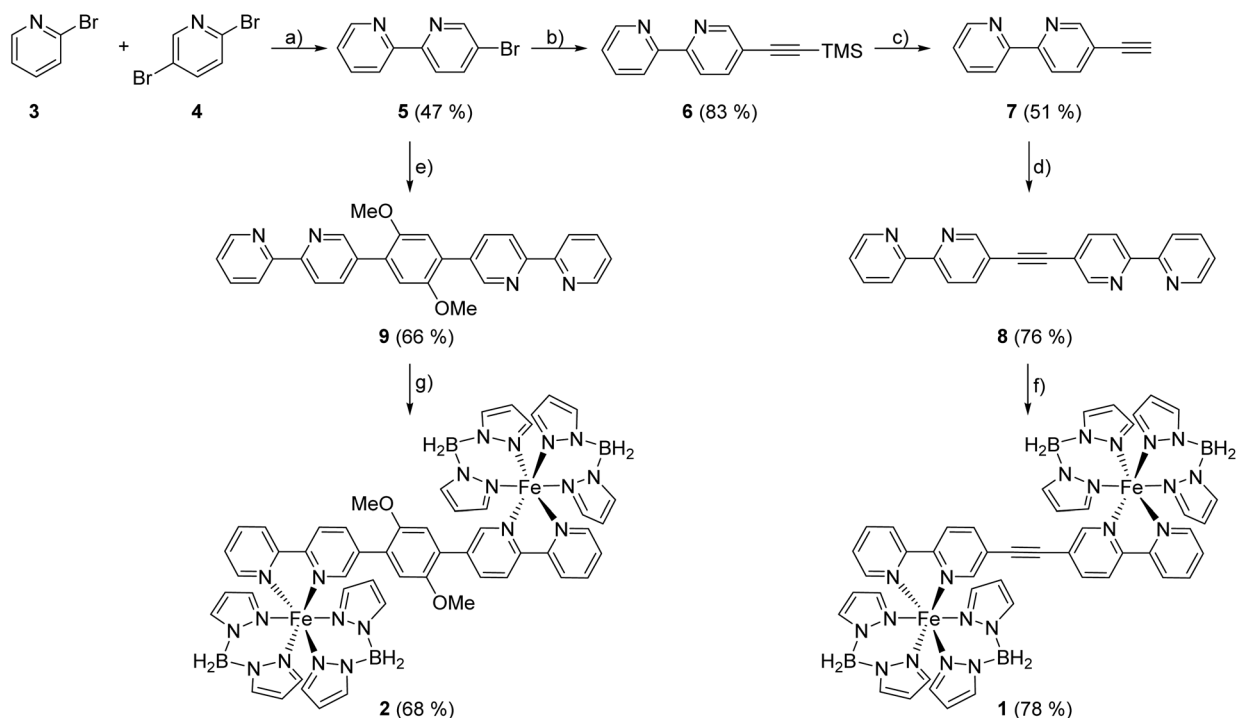
Results and discussion

Syntheses and characterisation

The bisbidentate bridging ligands 1,2-di(2,2′-bipyridine-5-yl)-ethyne (**8**, ac(bipy)₂) and 1,4-di(2,2′-bipyridine-5-yl)-3,5-dimethoxybenzene (**9**, Ph(OMe)₂(bipy)₂) are derived from 5-bromo-2,2′-bipyridine **5** which is synthesized by a Negishi cross-coupling reaction of 2,5-dibromopyridine (**4**) and 2-bromopyridine (**3**), following a general procedure of Luzung et al. for reactions of this type.[31] Suzuki cross-coupling of **5** with 1,4-diiodo-2,5-dimethoxyphenol then leads to Ph(OMe)₂(bipy)₂ (**9**) while for synthesis of ac(bipy)₂ (**8**) some more steps are needed. Following a modified procedure of Kim et al., bromo-bipyridine **5** is coupled with TMSA in a Sonogashira cross-coupling reaction to form 5-((trimethylsilyl)ethinyl)-2,2′-bipyridine (**6**) which is then deprotected to get the free acetylene **7**, allowing Sonogashira cross-coupling with bromobipyridine **5** to give the desired acetylene-bridged bisbipyridine ligand **8** (Scheme 1).[29] For preparation of the dinuclear complexes [Fe{(H₂B(pz)₂)₂}₂ μ-ac(bipy)₂] (**1**) and [Fe{(H₂B(pz)₂)₂}₂ μ-Ph(OMe)₂(bipy)₂] (**2**) (displayed in Scheme 1, bottom) the precursor complex [Fe(H₂B(pz)₂)₂(MeOH)₂], the synthesis of which seems to need methanol as solvent,[32] is prepared first, isolated and redissolved in tetrahydrofuran. Due to the poor solubility of the bridging ligands **8** and **9** in methanol they are added as solution (for **9**) or suspension (for **8**) in tetrahydrofuran.

Both coordination compounds **1** and **2** form as green precipitates, whereby coordination of Ph(OMe)₂(bipy)₂ (**9**) seems to take longer than reaction with ac(bipy)₂ (**8**). Hence, for **9** a longer reaction time is needed to get comparably good yields. This may originate from poorer coordination properties of this ligand due to steric hindrance of the methoxy groups.

The iron(ɪɪ) compounds **1** and **2** have been characterized by elemental analysis (ESI†). Also, BH₂ vibrations of the co-

Scheme 1 Synthesis of bisbipyridine based bridging ligands **8** and **9** and corresponding dinuclear compounds **1** and **2**: (a) i-PrMgCl, ZnCl₂, [Pd(PPh₃)₄], THF, 0 °C → 65 °C, 23 h; (b) TMSA, CuI, [Pd(PPh₃)₂Cl₂], NEt₃, THF, RT, 23 h; (c) K₂CO₃, MeOH, RT, 3 h; (d) **5**, [Pd(PPh₃)₄], NEt₃, toluene, 100 °C, 68 h; (e) 1,4-diiodo-2,5-dimethoxyphenol, n-BuLi, B(OMe)₃, [Pd(PPh₃)₄], K₂CO₃, THF, H₂O, −78 C → 75 °C, 5 d, (f) Fe(OTf)₂, K[H₂B(pz)₂], **8**, MeOH/THF, RT, 45 min, (g) Fe(OTf)₂, K[H₂B(pz)₂], **9**, MeOH/THF, RT, 2.5 h.

ordinated bispyrazolylborate in the IR spectra of **1** and **2** give strong evidence for the successful synthesis. On the other hand, **1** contains an acetylene group and therefore a perfect marker for vibrational spectroscopy. As expected for a molecule with a center of inversion, the symmetric stretching mode of the C≡C triple bond is not visible in the IR, but in the Raman spectrum, thus indicating the presence of a dinuclear complex (ESI, Fig. 1†).

Magnetic measurements

To investigate the magnetic properties of **1** and **2**, PPMS measurements were performed. As shown in Fig. 1 complexes **1** and **2** exhibit $\chi_M T$ values of 6.74 cm³ K mol⁻¹ and 5.99 cm³ K mol⁻¹ at 300 K, respectively, which is in the expected range for dinuclear iron(II) complexes in the HS–HS state.[33,34] The ethynyl-bridged bisbipyridine complex **1** shows a complete SCO (Fig. 1a). Upon lowering the temperature from 300 K, the transition starts at *ca.* 200 K and reaches a minimal $\chi_M T$ value of 0.35 cm³ K mol⁻¹ at *ca.* 65 K. In contrast, **2** shows an incomplete SCO roughly between 270 K and 63 K, which is rather gradual and finishes at a minimum $\chi_M T$ value of *ca.* 2.5 cm³ K mol⁻¹ (Fig. 1b). Below 20 K, both compounds exhibit a further decrease of $\chi_M T$, likely due to zero-field splitting of the Fe(II) high spin ground state.[21,35] Plotting the molar high spin fractions as a function of the temperature (Fig. 1c; black line) gives $T_{1/2} = 125$ K for **1**. The incomplete SCO of **2** exhibits an inflection point at 152 K and ends at 42% high spin fraction below 65 K (Fig. 1c; dark grey line).

Notably, the transition temperatures of the dinuclear compounds **1** and **2** are lower than for the related mononuclear complex [Fe(H₂B(pz)₂)₂(bipy)], which shows $T_{1/2} = 161$ K (light grey line in Fig. 1c).[15,16] This may be explained by a decreased nucleophilicity of the bisbipyridine ligands when coordinating two iron centres; *i.e.*, the coordination of the first Fe(II) ion already withdraws electron density from the ligand, resulting in a weaker ligand field upon coordination of the second iron

(II) center. Further, the dinuclear compounds **1** and **2** exhibit a more gradual and even incomplete SCO compared to the mononuclear parent compound [Fe(H₂B(pz)₂)₂(bipy)]. This corresponds to a decrease of cooperative behaviour. Specifically, the π–π stacking between the aromatic systems of the bipyridine units, which contribute to enhanced cooperativity in the bulk material,[19] might be hindered in the dinuclear compounds where the presence of two [Fe(H₂B(pz)₂)₂] units in the dimers impedes closer packing.[21,36]

Mössbauer spectroscopy

To complement the magnetic data, Mössbauer spectra of **1** and **2** were measured (Fig. 2). The spin-crossover behaviour of these compounds is clearly evident from the spectrum of **2** at 80 K which exhibits two doublets assignable to the HS and LS state (Fig. 2a). By contrast, the spectrum of **1** at 80 K (Fig. 2i) shows a dominant doublet typical for a Fe(II) LS–LS pair[15] (δ_{IS} = 0.41 mm s⁻¹; ΔE_Q = 0.49 mm s⁻¹) along with a low-intensity doublet (δ_{IS} = 1.08 mm s⁻¹; ΔE_Q = 2.56 mm s⁻¹) from the remaining HS–HS fraction (6%). The 300 K spectrum of **1** (Fig. 2j) exhibits one doublet with a quadrupole splitting of ΔE_Q = 2.10 mm s⁻¹ and an isomer shift of δ_{IS} = 0.92 mm s⁻¹, indicating the presence of a HS–HS pair. No subspectrum of the LS state is present, indicating γ_{HS} (**1**) = 1 at 300 K.

The two doublets of the 80 K spectrum of **2** (Fig. 2a) have an intensity ratio of 43 : 58 whereby the larger fraction corresponds to the LS (δ_{IS} = 0.42 mm s⁻¹; ΔE_Q = 0.65 mm s⁻¹) and the smaller fraction to the HS state (δ_{IS} = 1.05 mm s⁻¹; ΔE_Q = 2.76 mm s⁻¹). The slightly asymmetric appearance of both HS–HS doublets is caused by weak texture effects.[15] More striking, however, is the fact that the line width of the HS doublet is much larger than for the LS state.

To investigate the temperature dependence of the line-width, a series of spectra was measured for **2** at different temperatures between 300 K and 80 K. It turned out that the line-widths are more or less constant up to 200 K; *i.e.* no line-nar-
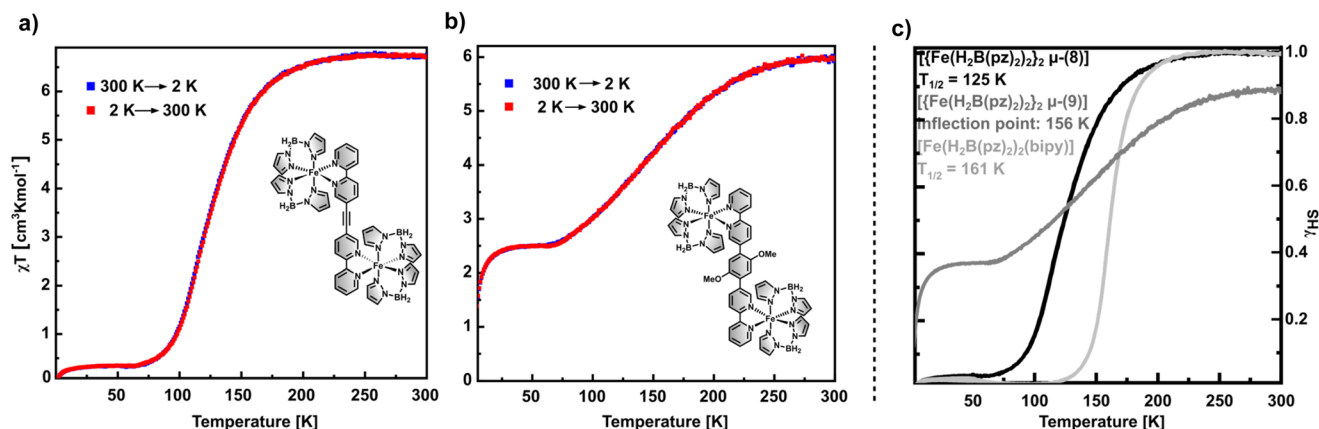

Fig. 1 For **1** (a) and **2** (b) $\chi_M T$ is plotted against the temperature showing that **1** undergoes a complete SCO while spin transition of **2** is incomplete and more gradual. For both compounds the cooling (blue dots) and heating (red dots) curves are identical. The right panel (c) compares the temperature-dependent high-spin fraction of the dinuclear compounds **1** (black line) and **2** (dark grey line) with the related mononuclear complex [Fe(H₂B(pz)₂)₂(bipy)] (light grey line), showing lower transition temperatures as well as more gradual transitions for the dinuclear complexes.

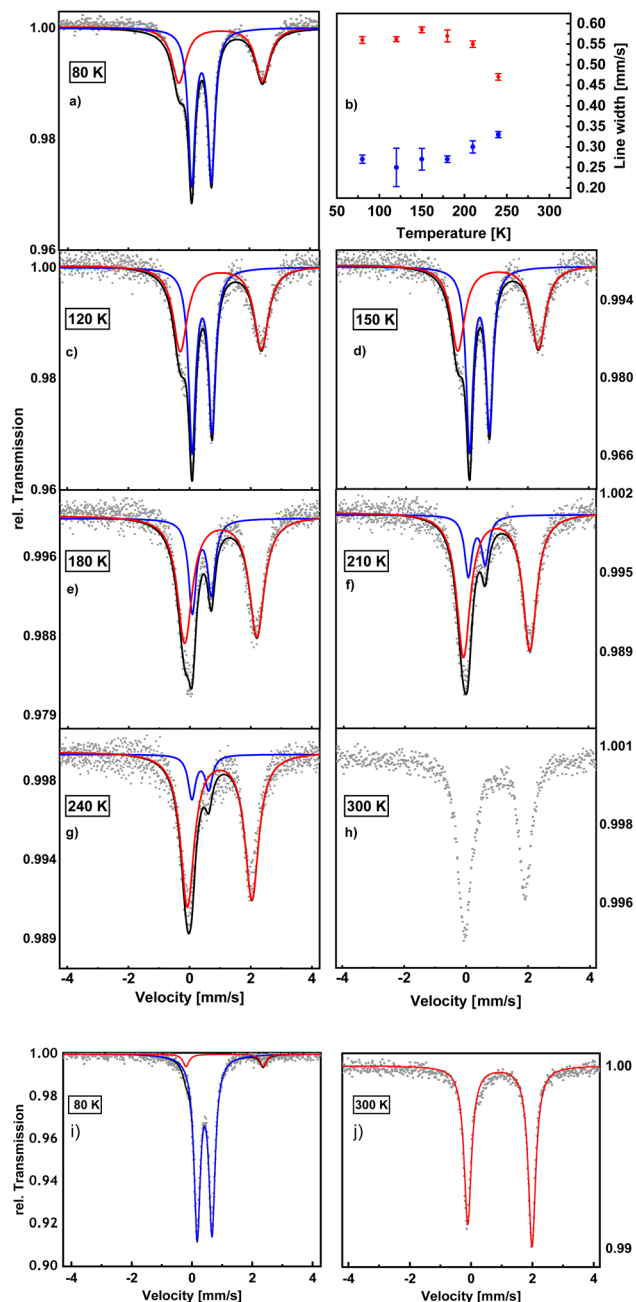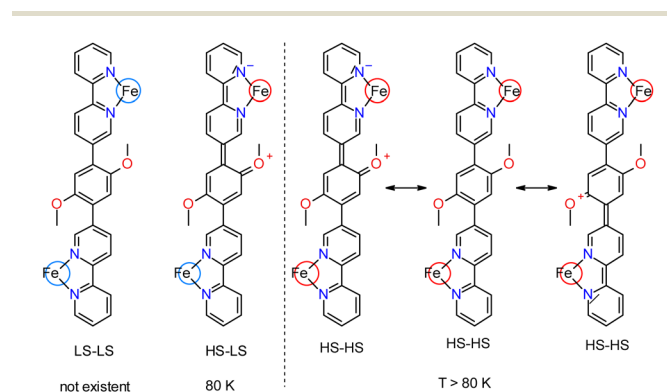**Fig. 2** Upper chart (a–h): Mössbauer spectra of [Fe{(H₂B(pz)₂)₂}₂ µ-Ph(OMe)₂(bipy)₂] (**2**) at temperatures between 80 K and 300 K. No systematic change of linewidths is observed upon variation of the temperature below 200 K (b). The asymmetry of the room-temperature quadrupole doublet is due to relaxation between the (dominant) HS state and a residual LS fraction. Lower Chart (i and j) Mössbauer spectra of [Fe{(H₂B(pz)₂)₂}₂ µ-ac(bipy)₂] (**1**) at 80 K (i) and 300 K (j) showing a HS−HS state at room temperature and a LS−LS state with 6% HS−HS residue at 80 K.

that of the LS spectrum increases, suggesting the onset of relaxation between HS and LS in this temperature range (see below).

The magnetic and Mössbauer data can be interpreted by assuming that below 80 K compound **2** adopts a HS–LS configuration whereby one iron center is locked in the HS state. Presumably, the HS spectrum is broadened by mesomerism of the bridging dimethoxyphenylene group, distorting the ligand environment around the HS Fe-center, but leaving the ligand sphere of the LS center intact. In the HS–LS state present at 80 K, therefore, the LS-doublet is sharp, in contrast to the HS doublet (Scheme 2). If the temperature is increased, the LS center undergoes a spin transition to HS. In the formed HS–HS state, mesomerism from the dimethoxyphenylene group can now be directed into either one of the two HS iron centers, giving rise to a distortion of the ligand environment and corresponding line broadening of the respective HS iron center, whereas the geometry of the other HS iron center stays intact (Scheme 2). In a static limit the resulting Mössbauer spectrum therefore is a superposition of a broad and a narrow HS-doublet. There can be relaxation between the two configurations in that the distorted and undistorted iron sites dynamically exchange their position (*cf.* Scheme 2, right). However, as the linewidth of the HS state stays more or less constant between 80 and 200 K (see above), a situation is obviously not reached within this temperature range where rapid fluctuation leads to a time-averaged coordination environment of the two HS-centers, which would be evident from a line-narrowing with respect to a static low-temperature situation.

The 300 K Mössbauer spectrum of compound **2** (Fig. 2h) also shows a broad HS doublet, but now this doublet is markedly asymmetric (in contrast to the spectra at lower temperatures) and no distinct LS spectrum can be identified any more.

Scheme 2 Schematic representation of the possible resonance structures of compound **2**. In the HS–LS state present at 80 K, the HS doublet is broad due to mesomerism of the bridging dimethoxyphenylene group into the HS center, distorting its coordination environment. In the HS–HS state being populated at *T* > 80 K, the compound may switch between different configurations in which one iron center is distorted and the other one not, giving rise to a superposition of a broad and a narrow HS-doublet. In the LS–LS state, which does not exist for compound **2**, no delocalization of charge from the bridging dimethoxyphenylene group into the iron center(s) occurs.

rowing of the broad HS doublet occurs between 80 to 200 K (Fig. 2b; ESI Table 1†). This indicates that within this temperature range the broadening of the HS state is not due to relaxation, but rather represents an intrinsic property of this state. Above 200 K, the linewidth of the HS spectrum decreases and

As a matter of fact, this spectrum is typical of a situation where relaxation occurs between a (dominant) Fe(II) HS state and a residual Fe(II) LS-fraction on the Mössbauer time scale.[37] Proper fitting of this spectrum requires the application of relaxation theory,[37] which is not available to us. We therefore refrain from fitting this spectrum.

Integration of the doublets provides information on HS : LS ratio (*cf.* ESI†) and, thus, on the HS fraction. Due to the fact that no fit of the 300 K-spectrum is possible in the static limit, an estimate of γ_{HS} (**2**) at 300 K was obtained from a comparison of the corresponding magnetic susceptibilities of **1** and **2** and γ_{HS} (**1**) = 1 at 300 K (see above). Based on the $\chi_M T$ values of 6.74 cm^3 K mol^{-1} for **1** and 5.99 cm^3 K mol^{-1} for **2**, it follows that γ_{HS} (**2**) = 0.89 at 300 K. The transition curves derived from Mössbauer spectroscopy and magnetic susceptibility measurements are compared in Fig. 3, showing overall agreement. Nevertheless, the thermal spin transition resulting from the Mössbauer data appears slightly steeper than that derived from the susceptibility data, and the inflection points of the corresponding curves differ by 4 K.

UV/Vis spectroscopy

To obtain further insight into the electronic structures and the SCO properties of **1** and **2**, both compounds were investigated by temperature-dependent UV/Vis spectroscopy. Fig. 4(a) shows UV/Vis spectra of **1** in KBr between 300 K and 80 K. The MLCT bands between 420 nm and 739 nm significantly increase in intensity upon cooling to 80 K, in agreement with the data obtained for the parent mononuclear complex [Fe(H$_2$B(pz)$_2$)$_2$(bipy)] (Fig. 4b).[16]

For **2** UV/Vis spectra could be obtained in KBr as well as in a polymer composite (polystyrene; *cf.* ESI†), which was not possible for **1** due to its poor solubility in any solvent. In both
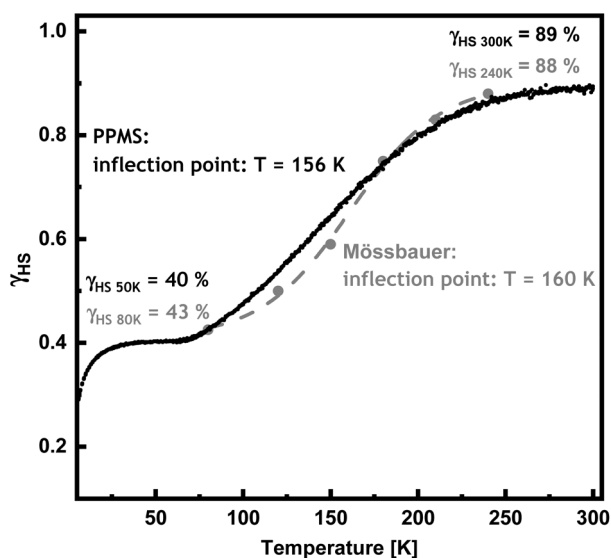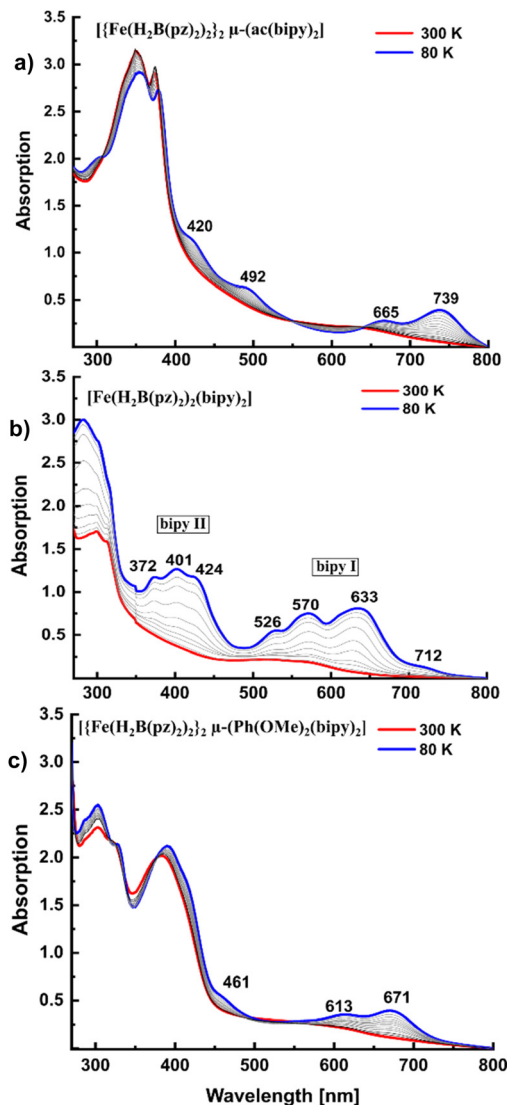
Fig. 4 Temperature dependent UV/Vis spectra of **1** crimped in KBr (a) and **2** in a polymer composite (polystyrene), (c) in comparison with the mononuclear parent compound [Fe(H$_2$B(pz)$_2$)$_2$(bipy)] (evaporated film on quartz glass) (b). The 300 K spectra are plotted in red, the 80 K spectra in blue and temperatures in between as grey lines. For [Fe(H$_2$B(pz)$_2$)$_2$(bipy)] (b) the "bipy I" and "bipy II" bands are indicated. The 712 nm band is assigned to a ^{3}MLCT transition (see text).

Fig. 3 Temperature-dependent HS fraction of [{Fe(H$_2$B(pz)$_2$)$_2$}$_2$ μ-(Ph(OMe)$_2$(bipy)$_2$)] (**2**) derived from Mössbauer spectroscopy (grey dots with grey dashed line) and PPMS measurements (black).

cases the 80 K spectra of **2** show significantly increased MLCT bands compared to the room temperature spectra (Fig. 4c), indicating SCO within this range. This is in good agreement with PPMS and Mössbauer data.

Temperature-dependent UV/Vis spectroscopy also allowed studies on the LIESST effect for **1** and **2**. Illumination with 617 nm at 5 K induces population of the metastable HS state for both compounds (Fig. 5a and b). While absorption does not decrease anymore after 5 min for **2**, it needs almost 2 h of illumination with 617 nm until conversion into the metastable high spin state is completed for **1**. On the other hand, when illuminated with 532 nm, LIESST is complete after 5 min for **1** as well (*cf.* ESI Fig. 2†). This seems reasonable in view of the
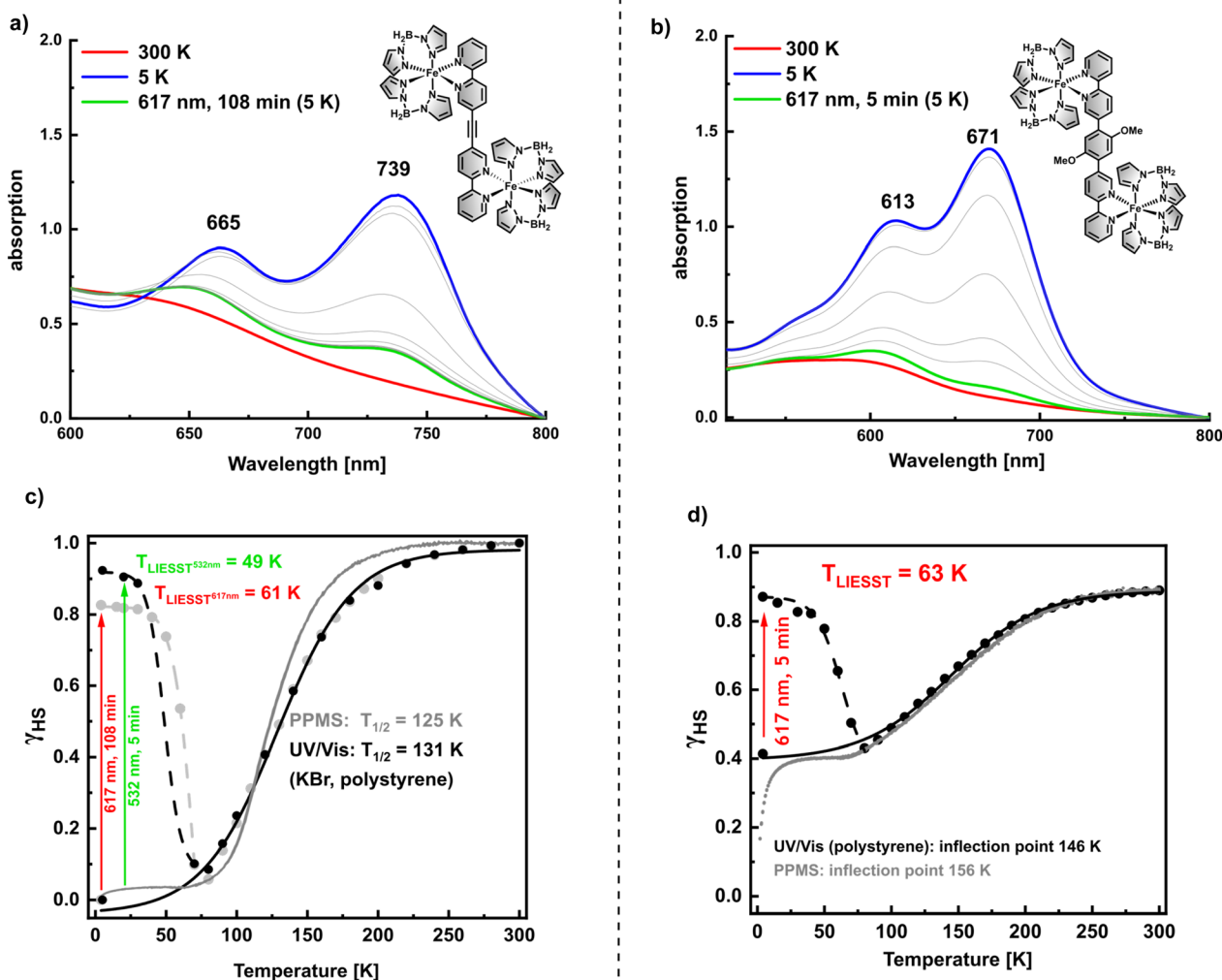
Fig. 5 LIESST measurements of **1** (a) and **2** (b) along with plots of resulting HS fraction as function of temperature (bottom): measurements were done at 300 K (red lines), 5 K (blue lines) and after illumination (green lines). Temperatures in between 5 K and 300 K are plotted as grey lines. (c) and (d): High spin fractions as function of temperature obtained from PPMS (dark grey line) and UV/vis data with Boltzmann fit (black/light grey dots, black line) as well as LIESST, shown by red/green arrows, and thermal relaxation (black/light grey dots, dashed black/light grey line) for complexes **1** (c) and **2** (d). **1** was measured as a KBr pellet coated with polystyrene to protect it from moisture, **2** was measured as a polymer composite (PS).

fact that LIESST proceeds through excitation in a MLCT state before relaxation into the HS state.[38] There is no absorption band at 617 nm in the UV/Vis spectrum of **1** while 532 nm lies in the MCLT band with a first maximum at 492 nm (Fig. 4a).

For comparison with the magnetic susceptibility data of **1** the absorption at 739 nm was converted into molar high-spin fraction *via* the equation

$$\gamma_{HS}(T) = \frac{OD_\lambda(T \to 0)}{\Delta OD_\lambda}\left(1 - \frac{OD_\lambda(T)}{OD_\lambda(T \to 0)}\right) \quad (1)$$

$\Delta OD_\lambda = OD_\lambda(T \to 0) - OD_\lambda(T \to \infty)$. The resulting plot is shown in Fig. 5c. The transition temperature $T_{1/2} = 132$ K derived from UV/Vis spectroscopy differs by 8 K from $T_{1/2} = 124$ K derived from PPMS. Further, the transition curve obtained by PPMS is more abrupt than the curve obtained from UV/Vis,

which may be due to reduced intermolecular interactions caused by grinding with KBr. LIESST is observed with an efficiency of 92% after illumination with 532 nm for 5 min and 82% by illumination with 617 nm for 108 min. Thermal relaxation into the LS state proceeds at T_{LIESST} (532 nm) = 49 K and T_{LIESST} (617 nm) = 61 K.

As shown by PPMS, SCO of **2** is incomplete at 5 K (see above). In order to get an impression of the spin transition obtained from UV/Vis spectroscopy, the absorption at 671 nm was converted into molar high spin fraction by eqn (1) employing γ_{HS} values of 0.43 at 80 K and 0.89 at 300 K (see above). Of course, there is no guarantee that SCO of compound **2** embedded in polystyrene exhibits the same γ_{HS} *vs.* *T* characteristics as the bulk material, but in this way LIESST efficiency can be approximately calculated and the UV/Vis and PPMS data become somewhat comparable.

As seen in Fig. 5d, LIESST also leads to a high-spin population of about 90% (532 nm). Thermal relaxation into the LS state proceeds at T_{LIESST} = 61 K. The inflection point of thermal SCO at 148 K is quite close to the inflection point obtained from PPMS measurements with 152 K. T_{LIESST} of the two dinuclear complexes **1** and **2** are close to values found for related mononuclear complexes $[Fe(H_2B(pz)_2)_2(L)]$ which are around 60 K.[16,20,21]

Notably, the MLCT bands of **1** and **2** are shifted by around 80–100 nm to lower energy compared to $[Fe(H_2B(pz)_2)_2(bipy)]$ (**Fehler! Verweisquelle konnte nicht gefunden werden.** b).[16,18,21] By comparing the spectra of the dinuclear compounds **1** and **2** it can be seen that **1** shows absorption maxima at even higher wavelengths than **2**. These shifts are explainable by considering the energies of the involved orbitals, in particular the bipyridine π* orbitals. As the bisbidentate bridging ligands have a significantly larger π-network and therefore a higher π-conjugation than one single bipyridine, lower lying π* orbitals are expected. Thus, the energy gap between metal and ligand π* orbitals is lower in the dinuclear compounds than in the mononuclear analogue and a shift of the MLCT bands to higher wavelengths is understandable.

The UV/vis spectrum of $[Fe(bipy)_3]^{2+}$ has intensively been studied by Gawelda *et al.*[39] and others, explaining that it contains two sets of MLCT transitions into bipyridine orbitals around 350 nm ("bipy I") and 500 nm ("bipy II").[40] The energy difference between these two bands roughly corresponds to the energy difference between the π* orbitals of bipyridine. Importantly, the UV/vis spectrum of $[Fe(H_2B(pz)_2)_2(bipy)]$ in the LS state is comparable to that of $[Fe(bipy)_3]^{2+}$, and the same band systems are observed (Fig. 4b). To identify the ^{3}MLCT band centred around 520 nm, Gawelda *et al.* fitted the absorption spectrum of aqueous $[Fe(bipy)_3]^{2+}$ in the region of the ^{1}MLCT band with a Franck–Condon progression of the high frequency skeleton mode of bipy at 1607 cm^{-1} (ν(C–N)/C–C), showing good agreement. For $[Fe(H_2B(pz)_2)_2(bipy)]$ this bipy skeleton mode is measured at an almost similar frequency (1595 cm^{-1}),[20,21,41] and the pattern is very similar to the ^{1}MLCT transition in $[Fe(bipy)_3]^{2+}$. Additionally, the spectrum of $[Fe(H_2B(pz)_2)_2(bipy)]$ shows a shoulder at the low energy tail of the ^{1}MLCT band (712 nm), which does not appear in the $[Fe(bipy)_3]^{2+}$ spectrum. Auböck *et al.* expect ^{3}MLCT bands between 600 nm and 700 nm for $[Fe(bipy)_3]^{2+}$,[40] so the shoulder at 712 nm could have its origin in a ^{3}MLCT transition. In the better resolved 10 K spectrum there are even some bands visible in between the ^{1}MLCT bands (555 nm, 607 nm, ESI Fig. 3†). Therefore, the bands centred around 570 nm are probably an overlap of progressions of ^{3}MLCT and ^{1}MLCT bands.

Vibrational spectroscopy

FIR. FIR spectra (500–200 cm^{-1}) of **1** and **2** were measured at 10, 100 and 300 K (Fig. 6). The 10 K and 300 K spectra of **1** show significantly different bands, reflecting the presence of a HS state at RT and a LS state at 10 K (Fig. 6a). The spectrum at 100 K (black line) contains bands of both states which is also not surprising in view of a $T_{1/2}$ of 125 K, determined by PPMS measurements, and a nonvanishing HS fraction at 100 K. By contrast, the spin transition of **2** is incomplete with a HS fraction of 42% at low temperatures (see above). Correspondingly, it is difficult to observe a clean spin transition of **2** *via* vibrational spectroscopy. Indeed, the HS bands remain visible at 10 K, and the temperature-dependent FIR spectra of **2** appear almost unchanged (Fig. 6b). This also confirms the
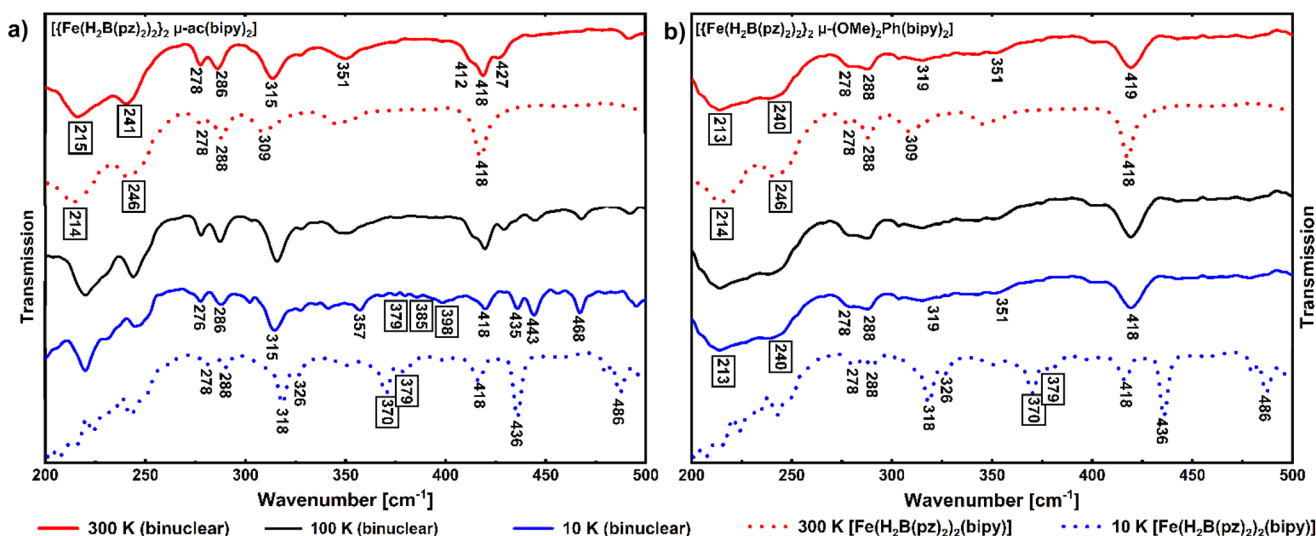

Fig. 6 FIR spectra of the dinuclear compounds **1** (a) and **2** (b) at 300 K (red lines), 10 K (blue lines) and 100 K (black lines) in comparison with the parent compound $[Fe(H_2B(pz)_2)_2(bipy)]$ (dotted lines). The complete SCO of **1** is apparent as the 10 K and 300 K spectra differ. Characteristic HS and LS modes appear in a similar region as observed for the mononuclear compound $[Fe(H_2B(pz)_2)_2(bipy)]$; they are marked with black boxes. The temperature dependent spectra of **2** appear all the same, reflecting the incomplete spin transition. As there is a HS fraction of 42% at low temperatures, modes of the HS state appear at all temperatures, while there are now characteristic LS bands observable.

observations from PPMS and Mössbauer spectroscopy that the HS–LS state of **1** present at 80 K does not undergo a transition to the LS–LS state upon further lowering the temperature.

The Fe–N stretching modes should shift to higher wavenumbers from the HS to the LS state.[42,43] That this is indeed the case has also been shown in studies of the parent complex $[Fe(H_2B(pz)_2)_2(bipy)]$ by comparing experimentally determined Fe–N stretching frequencies with theoretical ones. Thereby, characteristic HS bands have been identified at 214 cm^{-1} and 246 cm^{-1} as well as an intense band at 218 cm^{-1}, whereas the LS spectra show Fe–N stretching vibrations at 370 cm^{-1} and 379 cm^{-1}, along with less characteristic bands around 320 cm^{-1} and two intense bands at 436 cm^{-1} and 486 cm^{-1}.[35] Based on these data, a similar behavior of the dinuclear compounds **1** and **2** can be assumed, with spin-state-specific bands expected above 350 cm^{-1} in the spectrum for LS and below 250 cm^{-1} for HS. Indeed, the 300 K spectrum of compound **1** shows the same characteristic HS bands at 241 and 215 cm^{-1} (ν_{as}(Fe–N)) as reported for the mononuclear compound $[Fe(H_2B(pz)_2)_2(bipy)]$ in the HS state (Fig. 6a). Correspondingly, in the 10 K spectra, there are bands appearing in the region between 370 cm^{-1} and 400 cm^{-1} like in the mononuclear complex in the LS state.

While the spectra of compounds **1** and **2** and mononuclear $[Fe(H_2B(pz)_2)_2(bipy)]$ are nearly identical between 200 cm^{-1} and 350 cm^{-1}, there are some differences at higher wavenumbers. *e.g.*, due to more possible C–C vibrations in the bridging bisbipyridine ligand of the dinuclear compounds, the intense band at 418 cm^{-1} in the HS spectrum of $[Fe(H_2B(pz)_2)_2(bipy)]$ splits into three signals in the HS spectrum of **1** and develops into a broad signal for **2**. Furthermore, a higher number of bands in the LS spectrum of **2** above 418 cm^{-1} is observed.

Resonance Raman

For further investigation of the vibrational characteristics, resonance Raman spectroscopy was applied.[44,45] Based on its complete SCO behaviour, we focused on compound **1**. Raman spectra recorded at 300, 140 and 10 K with an excitation wavelength of 532 nm are given in Fig. 7(a). The overview spectra primarily exhibit peaks in the region of intraligand modes whereas peaks below 750 cm^{-1} (which should be more sensitive to the spin state) are barely visible. Nevertheless, some spectroscopic changes can be observed, but these mainly correspond to variations of absolute or relative intensities. The latter, *e.g.*, refers to the two peaks at 1140 and 1156 cm^{-1} (300 K) which shift to 1134 and 1154 cm^{-1} at 10 K. Conspicuously, also peaks at 777 and 1533 cm^{-1} become much more intense upon cooling, and new peaks at 1227 and 1429 cm^{-1} emerge.

Magnification of the spectral region below 750 cm^{-1} is shown in Fig. 7(b) for 300 K (where HS should be present) and 75 K (where the LS should be dominant; additional data at 140 K and 10 K given in the ESI, Fig. 2†). Clearly, a peak at 393 cm^{-1} appears in the 75 K spectrum which is not present in the room-temperature spectrum. A peak at this position has been assigned to a Raman-active metal–ligand vibration of the LS state in $[Fe(H_2B(pz)_2)_2(phen)]$.[46] Moreover, a new peak emerges at 642 cm^{-1} in the 75 K spectrum of **1**; a peak at a similar position has been attributed to a LS vibration of $[Fe(H_2B(pz)_2)_2(phen)]$ as well.[46] Comparing the 300 and 75 K spectra of compound **1**, on the other hand, it is not easy to identify the Raman-active metal–ligand vibration(s) of the HS state which should appear between 200 and 250 cm^{-1} and vanish in the LS state (see above). The 10 K spectrum of **1**, finally, contains peaks of the 300 K HS-spectrum (albeit with
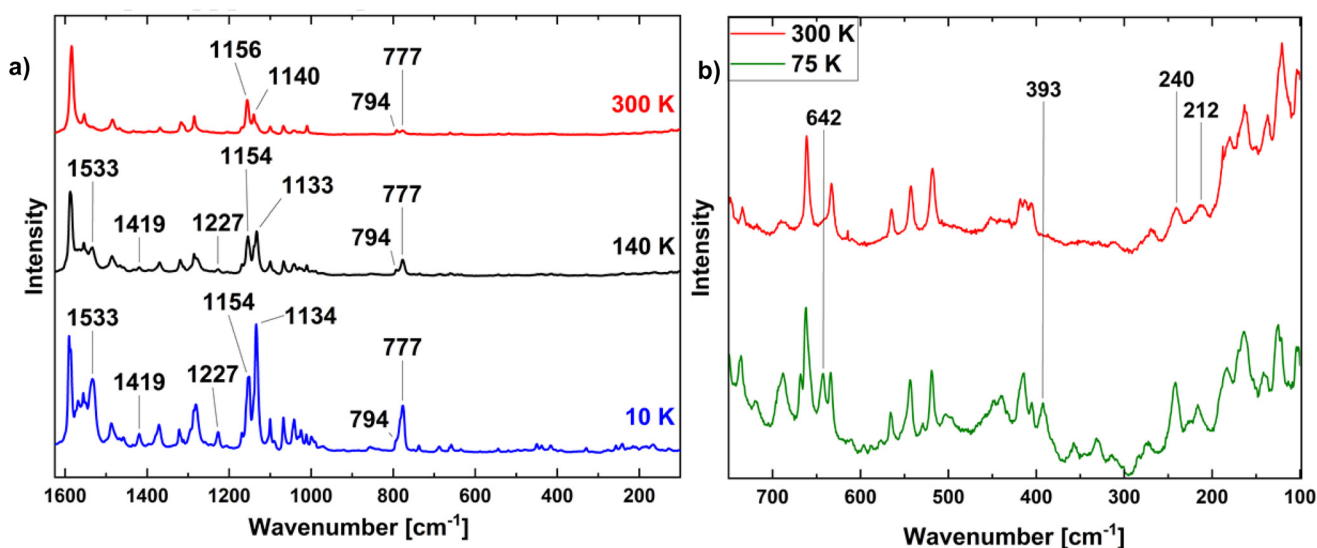

Fig. 7 (a) Resonance Raman spectra of the dinuclear compound **1** at different temperatures. All samples where measured with 532 nm. (b) Spectra of the region 100–750 cm^{-1}. Positions of HS-peaks (300 K) disappearing upon cooling and LS-peaks (75 K) emerging at low temperature are indicated.

modified intensities) along with other peaks not present in the 300 K spectrum. It is probably affected by (at least partial) excitation of the molecules to the HS state through irradiation with the Raman laser (*cf.* ESI Fig. 4†).[46] The presence of additional peaks might indicate a distortion of the complex at low temperatures. In the Raman spectra of **2** recorded at 300 K, 100 K and 10 K no significant differences can be identi-

fied (see ESI Fig. 5†). This, however, can be explained with the coexistence of both spin states at low temperatures, which is also indicated by the PPMS measurements (see above).

X-ray absorption spectroscopy

Compound **1** has further been examined by X-ray absorption spectroscopy (XAS). To determine the temperature-induced

Fig. 8 (a): XAS-spectra of **1**, temperature-dependent measurement from 10 K to 300 K at the L$_3$ edge of Fe. (b): γ_{HS} as function of temperature with fitted van't Hoff equation. (c) SOXIESST measurements at 10 K (d) γ_{HS} of **1** induced by X-ray illumination fitted with eqn (3). (e): XAS spectra of **1**, LIESST measurements at a sample temperature of 10 K, illumination with 520 nm laser. (f): γ_{HS} light-induced at 10 K, SOXIESST overlay calculated using c, r_x, k from SOXIESST and time of scan.

switching of **1**, the sample was first cooled down to 10 K and heated up to 300 K again (Fig. 8a). The spectra in this Figure are recorded with the molecules in thermal equilibrium. The data reflect a spin-state switching of **1** by heating from 10 K to 300 K. The spectrum at 270 K with main peak at 706.5 eV shows primarily the HS state of the molecules, while at 50 K the main peak at 707.9 eV shows primarily the LS state of **1**.[22]

A comparison of the XAS spectrum of **1** at 300 K with that of the parent mononuclear complex[15] indicates that some fraction of molecules stays in the LS state. To calculate the HS fraction a least squares fit has been performed by taking the reference HS and LS spectra at 300 K and 75 K, respectively, of a 10 ML thin film of the mononuclear complex.[19] The fit of the spectra at 300 K and 50 K shows that 87% of the complex is in the HS state at 300 K and around 25% of the complex is in the HS state at 50 K. Thus, 63% of the molecules are switching with temperature.

The high-spin fraction γ_{HS} for the thermal equilibrium between HS and LS can be calculated using the van't Hoff equation:[9]

$$\gamma_{HS} = x + (1-x)(\exp(\Delta H/RT - \Delta S/R) + 1)^{-1} \qquad (2)$$

where x is the fraction of molecules locked in HS state, ΔH is the enthalpy difference between HS and LS and R the gas constant. The fit in Fig. 8b with the parameters $\Delta H = 5.4(7) \times 10^3$ J mol^{-1} and $\Delta S = 43.9(6)$ J K^{-1} mol^{-1} yields $T_{1/2} \approx 122$ K, which is in good agreement with the PPMS measurements (see above, Fig. 1).

Notably, the thermodynamic parameters are similar to those of the parent molecule [Fe(H$_2$B(pz)$_2$)$_2$(bipy)] with $\Delta H = 7.7$ kJ mol^{-1}, $\Delta S = 47.4$ J K^{-1} mol^{-1} obtained by Moliner *et al.*[15] This indicates that the interaction between the two iron centers is comparatively weak.

Importantly, the spectrum at 10 K reveals the SOXIESST effect (soft X-ray-induced excited spin-state trapping) on compound **1** which increases the HS fraction as compared to the 50 K spectrum.[22] The increase in the γ_{HS} value below 80 K clearly indicates that the molecules are sensitive to X-rays. In order to quantify the rate for SOXIESST, compound **1** was measured at a sample temperature of 10 K under constant X-ray illumination (Fig. 8c). The illumination time is the accumulated scan time over the energy range of the Fe L$_3$ edge. The data in Fig. 8d can be fitted with:

$$\gamma_{HS} = c - \exp(-t_x \times r_x) \times k \qquad (3)$$

where c is the saturation level, t_x the time of X-ray illumination, r_x the rate constant and k a factor for the initial saturation. The initial saturation must be considered because of the sensitivity of the molecules to X-rays at low temperatures, which causes a switching during the scan. The parameters of the fit in Fig. 8d are: $r_x = 2.2(2) \times 10^{-3}$ s^{-1}, $c = 0.69(2)$ and $k = 0.36(1)$. The results show that 69% of the molecules switch to the HS state only by X-ray illumination. For comparison, the SOXIESST rate with the parent molecule at a similar X-ray flux, as 0.8 ML on

HOPG, is $r_x = 3.50(3) \times 10^{-4}$ s^{-1},[22] confirming the high sensitivity of **1** towards X-rays. Fig. 8e shows the spectra of compound **1** recorded after light illumination with 520 nm, which exhibit almost complete switching of the molecules from HS to LS. The sample was not exposed to X-rays during illumination with light. In Fig. 8f the evaluated γ_{HS} for the corresponding illumination time is shown.

Excitation to the LIESST state cannot be determined reliably because of the sensitivity of **1** to X-rays and the high flux of the beamline, the scanning time of ≈120 s per scan and the unknown SOXIESST relaxation rate at low temperatures. Qualitatively, however, it can be seen that the light-induced high-spin fraction comes close to 95% after about 2700 s while SOXIESST saturates at 69%, confirming that **1** is sensitive to photons with 520 nm wavelength. To obtain better data, further measurements with reduced X-ray flux will be carried out in our next possible beamtime experiment.

Conclusions

With the aim of analysing the effect of cooperativity, we connected two entities of the well-known and intensively examined complex [Fe(H$_2$B(pz)$_2$)$_2$(bipy)] by two different linkers to obtain the dinuclear spin crossover (SCO) complexes [{Fe(H$_2$B(pz)$_2$)$_2$}$_2$μ-(ac(bipy)$_2$)] (**1**) and [{Fe(H$_2$B(pz)$_2$)$_2$}$_2$μ-(Ph((OMe)$_2$(bipy)$_2$))] (**2**). The compounds and their spin-crossover properties were investigated through PPMS measurements, Mössbauer spectroscopy, vibrational as well as UV/Vis spectroscopy and X-ray absorption spectroscopy.

Compound **1**, bridged by an acetylene unit, exhibits a complete thermal SCO with a transition temperature ($T_{1/2}$) of 125 K, while compound **2**, with a bridging dimethoxyphenylene unit, shows an incomplete SCO with an inflection point at 152 K. The transition temperatures of these dinuclear compounds are lower than that of the mononuclear parent complex [Fe(H$_2$B(pz)$_2$)$_2$(bipy)], suggesting a decreased of ligand-field strength of the terminal bipy units due to dimer formation.

Mössbauer spectroscopy confirms the presence of HS–HS pairs in both compounds at 300 K, with compound **2** also showing a small LS fraction. At 80 K, compound **1** exhibits a LS–LS state along with a minor HS–HS fraction, while compound **2** displays two doublets of comparable intensity corresponding to a HS–LS state. The observation of broad HS doublets in the Mössbauer spectra of **2** at all temperatures is attributed to a mesomeric (+M) effect of the dimethoxyphenylene group directed into one Fe(II) HS center.

UV/Vis spectroscopy provided further insights into the SCO properties of the compounds, showing an increased intensity of the MLCT bands at lower temperatures, consistent with the LS state. These results complemented the findings from PPMS and Mössbauer experiments, confirming the occurrence of SCO in the studied dinuclear compounds.

Far-infrared spectroscopy showed a shift of Fe–N stretching vibrations to higher wavenumbers at low temperatures for **1**

while the spectra of **2** looked the same at all temperatures, also confirming the findings from PPMS measurements. The Raman spectra were less conclusive with respect to the presence of a spin transition. In any case, a peak at 393 cm^{-1} assignable to the low-spin state was detected for compound **1** at 75 K. Going to lower temperatures, the Raman spectra are probably affected by the LIESST effect, due to (at least partial) excitation to the metastable high-spin state in a thermal region where the low-spin state is expected.

Compound **1** was further examined by X-ray absorption spectroscopy (XAS), also showing a thermal SCO in bulk form. XAS studies on LIESST showed complete switching from LS to HS state at 10 K with light illumination, although there is significant contribution to the HS state due to the SOXIESST effect, which makes it challenging to determine the exact LIESST rate.

Overall, the data reflect a reduced cooperativity of the spin transitions exhibited by **1** and **2** with respect to the parent mononuclear complex [Fe(H$_2$B(pz)$_2$)$_2$(bipy)]. While this may be surprising, it can be attributed to the steric hindrance, limiting closer packing and reducing intermolecular interactions such as π–π stacking which are important factors for the cooperative behaviour observed for the parent mononuclear complex.[47]

Conflicts of interest

There are no conflicts to declare.

Acknowledgements

References

1 P. Gütlich, A. Hauser and H. Spiering, *Angew. Chem., Int. Ed. Engl.*, 1994, **33**, 2024.

2 P. Gütlich, A. B. Gaspar and Y. Garcia, *Beilstein J. Org. Chem.*, 2013, **9**, 342.

3 J. A. Real, A. B. Gaspar and M. C. Muñoz, *Dalton Trans.*, 2005, **34**, 2062.

4 O. Kahn and C. J. Martinez, *Science*, 1998, **279**, 44.

5 E. Collet and P. Guionneau, *C. R. Chim.*, 2018, **21**, 1133.

6 J. A. Real, A. B. Gaspar, V. Niel and M. C. Muñoz, *Coord. Chem. Rev.*, 2003, **236**, 121.

7 K. S. Murray, *Eur. J. Inorg. Chem.*, 2008, **2008**, 3101–3121.

8 J. R. Galán Mascarós, G. Aromí and M. Darawsheh, *C. R. Chim.*, 2018, **21**, 1209.

9 A. Hauser, J. Jeftić, H. Romstedt, R. Hinek and H. Spiering, *Coord. Chem. Rev.*, 1999, **190**, 471.

10 N. Willenbacher and H. Spiering, *J. Phys. C: Solid State Phys.*, 1988, **21**, 1423.

11 H. Spiering, J. Linares and F. Varret, *Phys. Rev. B: Condens. Matter Mater. Phys.*, 2004, **70**, 184106.

12 A. B. Gaspar, M. C. Muñoz and J. A. Real, *J. Mater. Chem.*, 2006, **16**, 2522.

13 K. S. Murray and C. J. Kepert, *Top. Curr. Chem.*, 2004, **233**, 195.

14 O. Kahn, J. Kröber and C. Jay, *Adv. Mater.*, 1992, **4**, 718.

15 N. Moliner, L. Salmon, L. Capes, M. C. Muñoz, J.-F. Létard, A. Bousseksou, J.-P. Tuchagues, J. J. McGarvey, A. C. Dennis, M. Castro, R. Burriel and J. A. Real, *J. Phys. Chem. B*, 2002, **106**, 4276.

16 H. Naggert, A. Bannwarth, S. Chemnitz, T. Von Hofe, E. Quandt and F. Tuczek, *Dalton Trans.*, 2011, **40**, 6364.

17 S. Ossinger, H. Naggert, L. Kipgen, T. Jasper-Toennies, A. Rai, J. Rudnik, F. Nickel, L. M. Arruda, M. Bernien, W. Kuch, R. Berndt and F. Tuczek, *J. Phys. Chem. C*, 2017, **121**, 1210.

18 M. Bernien, H. Naggert, L. M. Arruda, L. Kipgen, F. Nickel, J. Miguel, C. F. Hermanns, A. Krüger, D. Krüger, E. Schierle, E. Weschke, F. Tuczek and W. Kuch, *ACS Nano*, 2015, **9**, 8960.

19 L. Kipgen, M. Bernien, S. Ossinger, F. Nickel, A. J. Britton, L. M. Arruda, H. Naggert, C. Luo, C. Lotze, H. Ryll, F. Radu, E. Schierle, E. Weschke, F. Tuczek and W. Kuch, *Nat. Commun.*, 2018, **9**, 2984.

20 H. Naggert, J. Rudnik, L. Kipgen, M. Bernien, F. Nickel, L. M. Arruda, W. Kuch, C. Näther and F. Tuczek, *J. Mater. Chem. C*, 2015, **3**, 7870.

21 S. Ossinger, L. Kipgen, H. Naggert, M. Bernien, A. J. Britton, F. Nickel, L. M. Arruda, I. Kumberg, T. A. Engesser, E. Golias, C. Näther, F. Tuczek and W. Kuch, *J. Phys.: Condens. Matter*, 2020, **32**, 114003.

22 L. Kipgen, M. Bernien, F. Nickel, H. Naggert, A. J. Britton, L. M. Arruda, E. Schierle, E. Weschke, F. Tuczek and W. Kuch, *J. Phys.: Condens. Matter*, 2017, **29**, 394003.

23 E. Ludwig, H. Naggert, M. Kalläne, S. Rohlf, E. Kröger, A. Bannwarth, A. Quer, K. Rossnagel, L. Kipp and F. Tuczek, *Angew. Chem., Int. Ed.*, 2014, **53**, 3019.

24 K. S. Kumar and M. Ruben, *Angew. Chem., Int. Ed.*, 2021, **60**, 7502.

25 V. Shalabaeva, S. Rat, M. D. Manrique-Juarez, A.-C. Bas, L. Vendier, L. Salmon and G. Molnár, *J. Mater. Chem. C*, 2017, **5**, 4419.

26 N. H. Damrauer, G. Cerullo, A. Yeh, T. R. Boussie, C. V. Shank and J. K. McCusker, *Chemtracts*, 1998, **11**, 621.

27 V. Grosshenny, F. M. Romero and R. Ziessel, *J. Org. Chem.*, 1997, **62**, 1491.

28 Y. R. Choi, W. Lee, S. H. Yun, H. Lee, J. Tak, B. Park and B. H. Kim, *Monatsh. Chem.*, 2017, **148**, 2051.

29 M. Kim, C. H. Kang, S. Hong, W.-Y. Lee and B. H. Kim, *Inorg. Chim. Acta*, 2013, **395**, 145.

30 N. Das, G. S. Bindra, A. Paul, J. G. Vos, M. Schulz and M. T. Pryce, *Chem. – Eur. J.*, 2017, **23**, 5330.

31 M. R. Luzung, J. S. Patel and J. Yin, *J. Org. Chem.*, 2010, **75**, 8330.

32 S. Ossinger, C. Näther and F. Tuczek, *IUCrData*, 2016, **1**, x161252.

33 J. A. Real, I. Castro, A. Bousseksou, M. Verdaguer, R. Burriel, M. Castro, J. Linares and F. Varret, *Inorg. Chem.*, 1997, **36**, 455.

34 A. B. Gaspar, V. Ksenofontov, V. Martinez, M. C. Muñoz, J. A. Real and P. Gütlich, *Eur. J. Inorg. Chem.*, 2004, **2004**, 4770.

35 S. Ossinger, H. Naggert, E. Bill, C. Näther and F. Tuczek, *Inorg. Chem.*, 2019, **58**, 12873.

36 S. Ossinger, C. Näther and F. Tuczek, *J. Phys.: Condens. Matter*, 2020, **32**, 094001.

37 P. Adler, H. Spiering and P. Gütlich, *Inorg. Chem.*, 1987, **26**, 3845–3850.

38 S. Decurtins, P. Gütlich, C. P. Köhler, H. Spiering and A. Hauser, *Chem. Phys. Lett.*, 1984, **105**, 1–4.

39 W. Gawelda, A. Cannizzo, V. T. Pham, F. Van Mourik, C. Bressler and M. Chergui, *J. Am. Chem. Soc.*, 2007, **129**, 8199.

40 G. Auböck and M. Chergui, *Nat. Chem.*, 2015, **7**, 629.

41 J. A. Real, M. C. Muñoz, J. Faus and X. Solans, *Inorg. Chem.*, 1997, **36**, 3008.

42 J. H. Takemoto and B. Hutchinson, *Inorg. Nucl. Chem. Lett.*, 1972, **8**, 769.

43 J. H. Takemoto and B. Hutchinson, *Inorg. Chem.*, 1973, **12**, 705.

44 Z. G. Lada, *Magnetochemistry*, 2022, **8**, 108.

45 C. Brady, P. L. Callaghan, Z. Ciunik, C. G. Coates, A. Døssing, A. Hazell, J. J. McGarvey, S. Schenker, H. Toftlund, A. X. Trautwein, H. Winkler and J. A. Wolny, *Inorg. Chem.*, 2004, **43**, 4289.

46 R. Sylvain, M. Mikolasek, J. Sánchez Costá, A. I. Chumakov, W. Nicolazzi, G. Molnár, L. Salmon and A. Bousseksou, *Chem. Phys. Lett.*, 2016, **653**, 131.

47 S. Ossinger, C. Näther, A. Buchholz, M. Schmidtmann, S. Mangelsen, R. Beckhaus, W. Plass and F. Tuczek, *Inorg. Chem.*, 2020, **59**, 7966–7979.